Performance Optimization of an InP-Based Widely Tunable All-Optical Wavelength Converter Operating at 40 Gb/s

Vikrant Lal, *Student Member, IEEE*, Milan L. Mašanović, *Member, IEEE*, Joseph A. Summers, *Student Member, IEEE*, Larry A. Coldren, *Fellow, IEEE*, and Daniel J. Blumenthal, *Fellow, IEEE*

***Abstract*—We report on the design and performance optimization of a quantum-well active region-based semiconductor optical amplifier Mach–Zehnder interferometer wavelength converter monolithically integrated with a widely tunable sampled-grating distributed Bragg reflector laser, operating differentially at 40 Gb/s. The device is fabricated using an offset quantum-well platform, requiring a single regrowth. We show error-free operation, with a less than 3-dB power penalty at the optimal differential delay, and open eyes across a 25-nm output tuning range.**

***Index Terms*—Mach–Zehnder interferometer (MZI), photonic integrated circuit, semiconductor optical amplifier (SOA), wavelength conversion, wavelength-division multiplexing.**

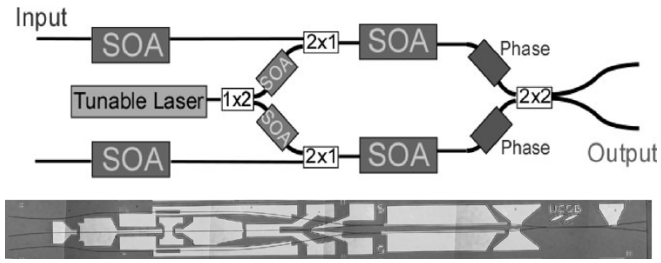

Fig. 1. Schematic of the device design showing the different components and a microscope image of the fabricated device.

I. Introduction

ULTRAHIGH capacity optical data routing systems are expected to form the backbone of future networks. The realization of such systems though, depends on significant reductions in power, footprint, and cost requirements. One key function in such systems will be all-optical wavelength conversion, due to the potential advantages it can offer such as increased connection flexibility, network capacity, ease of network management, and potential reduction in optical buffering requirements [1].

Monolithic integration of high-speed all-optical wavelength converters is a very important step toward meeting the cost requirements. Semiconductor optical amplifier (SOA)-Mach–Zehnder interferometer (SOA-MZI)-based integrated wavelength converters are a good candidate for systems operating at 40 Gb/s due to the ultrafast carrier-depletion-induced refractive index changes in an SOA. The maximum speed of the SOA-MZI converters is limited primarily by the carrier recovery lifetime in the SOAs. An attractive approach that has been previously demonstrated to overcome the SOA carrier recovery limitation, and is used in this letter, is a differential scheme in which the fast carrier-depletion in one arm is used to switch the MZI on, while the same fast carrier-depletion is used, after a suitable delay, in the other arm to turn it back off [2]–[5]. An optimized delay is crucial for the chip performance, and a detailed study on its influence of the converter performance, to the best of our knowledge, has not been published before.

In this letter, for our delay study, we used a differential 40-Gb/s widely tunable all-optical wavelength converter (TAO-WC) with on-board widely tunable sampled-grating distributed Bragg reflector (SG-DBR) laser fabricated in the offset quantum-well (OQW) platform [6]. The device schematic is shown in Fig. 1, along with a microscope image of the fabricated device. The dimensions of the fabricated device are 0.5×4.8 mm^2. The OQW integration platform offers a robust and simple high yield approach for high density integration of active–passive components on chip. The on-chip tunable laser source greatly simplifies the operation of the device and allows us to select the desired output wavelength from the converter in a fast and power efficient manner. We have previously demonstrated the operation of wavelength converters in the OQW platform operating at 10-Gb/s nonreturn-to-zero (NRZ) [6], [7]. The OQW platform offers an excellent approach for fabricating complex quantum-well-based low-power consumption photonic integrated circuits. One potential limitation of this platform is the low confinement factor that results due to the position of the quantum wells on top and not in the center of the waveguide [7].

For 40-Gb/s operation reported in this letter, the devices are redesigned to have shorter preamplifier SOAs (600 μm long) to reduce saturation and pattern-dependent effects while still providing adequate gain for the input signal. Also, for use in an external differential-delay-based configuration, two input waveguides are needed, which are then bent in opposite directions to allow easy coupling of two fibers to the input facet. We study the effect of the differential delay on the performance of the device and show that selection of the optimal delay is very important for this class of devices. The optimal delay value depends

Manuscript received July 15, 2005; revised November 23, 2005. This work was supported by the Defense Advanced Research Projects Agency (DARPA)/MTO DOD-N program under the LASOR Project Award W911NF-04-9-0001.

The authors are with the Electrical and Computer Engineering Department, University of California at Santa Barbara, Santa Barbara, CA 93106 USA (e-mail: lal@ece.ucsb.edu).

Digital Object Identifier 10.1109/LPT.2005.864000

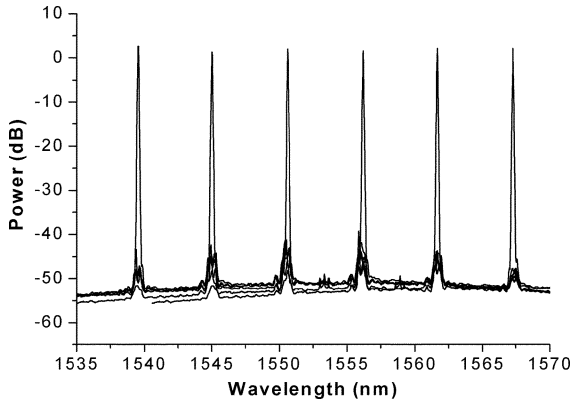

Fig. 2. Output tuning spectrum showing a few representative output wavelengths.

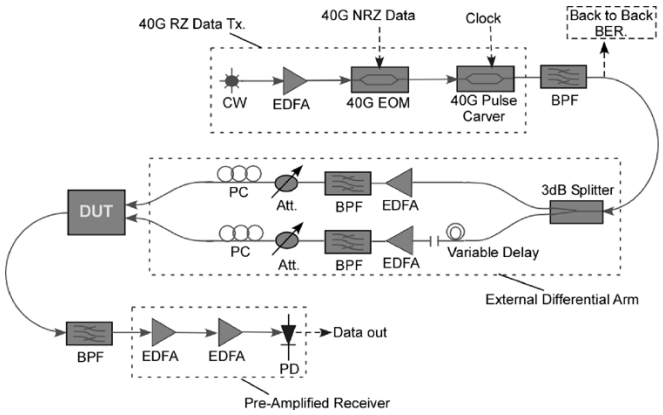

Fig. 3. A 40-Gb/s wavelength conversion experimental setup.

on the input pulsewidth and needs to be determined before the delay can be integrated on-chip.

We also demonstrate that error-free operation can be achieved at 40-Gb/s return-to-zero (RZ) with a less than 3-dB power penalty at the optimal delay value. The devices show clearly open eyes across an output wavelength tuning range of 25 nm, which is limited by the available erbium-doped fiber amplifier (EDFA) gain bandwidth in the receiver.

II. Device Design and Operation

The device consists of a widely tunable SG-DBR laser monolithically integrated with an SOA-MZI [7]. The on-chip tunable laser source greatly increases the functionality and efficiency of the device and simplifies the operation by providing a stable continuous-wave (CW) signal, and maintaining a fixed CW polarization state. Fig. 2 shows overlaid spectra from the SG-DBR laser at a few representative wavelengths. The laser itself can be continuously tuned over this entire range. The SOA-MZI has 1-mm-long SOAs in each branch. The SOA dimensions were chosen based on our previous experiments [7] to get a large phase swing in the MZI and fast SOA operation.

We characterize the effect of varying the differential delay on the performance of the device, and find that selection of a large enough delay is critical to the performance of the device. The optimal delay value is determined primarily by the input pulsewidth and needs to be optimized before the delay can be integrated on-chip. Fig. 3 shows the experimental setup for 40-Gb/s wavelength conversion using an external differential arm. The input signal is obtained by first modulating a CW source with 40-Gb/s NRZ data, generated using an SHF 40-Gb/s bit-error-rate tester (BERT). This signal is then converted to RZ format using a pulse carver to shape the pulses. The measurements in this letter are performed using pseudorandom binary sequence (PRBS) $2^{31}-1$ data. The resulting signal in our setup has a pulsewidth of 11 ps. The input signal is split into two paths, which are delayed with respect to each other; this delay can be controlled in order to control the output pulsewidth from the TAO-WC. The two versions of the input data are amplified using EDFAs and filtered using 2-nm filters to remove ASE and then coupled into the device by using two lensed fibers mounted on piezo-controlled translation stages, to couple to the two input arms of the MZI. The typical coupling loss for our setup is 4 dB. The input signal is amplified by using SOAs to get the desired signal power into the SOA-MZI. These preamplifier SOAs are among the critical components in these devices. The slow gain recovery in the preamplifiers leads to pattern dependence that can severely hamper the device performance. It is, therefore, very important to minimize the pattern dependence introduced by the preamplifier SOAs. Our current device design has 600-μm-long preamplifiers; the length was chosen to minimize patterning due to saturation effects, while still getting sufficient output power to drive the MZI. Further optimization of the preamplifier design for integrated high-speed tunable wavelength converters is a current topic of our research. The operating point of the wavelength converter is optimized by selecting the relative delay and gain of the arms. With proper selection of the relative gain and delay between the arms to balance the phase change, we use the fast carrier depletion process to turn the MZI ON and OFF [3]. The output signal of the device is filtered using a 1.2-nm-wide filter to remove the input signal wavelength and then sent through a preamplified receiver, as shown in Fig. 3, to a 50-GHz photodetector. The BER measurements are performed using an SHF 40-GHz BERT.

III. Device Performance

The delay between the pulses greatly influences the performance of the wavelength converter. Enough delay is needed to allow the MZI to achieve enough differential phase swing in the switching window. If the delay is too small, then the phase swing in the switching window is low and the output signal power is reduced, leading to excessive power penalty. It is expected that to allow for maximum phase swing, the differential delay should be similar to the input pulsewidth. A longer delay will not cause a larger eye-opening but will increase the output pulsewidth, and hence power, also leading to an increased penalty. The differential delay was varied from 6.67 to 13.33 ps, and BER measurements were performed. Fig. 4(a) shows the BER curves obtained at different delay values. We see that as the delay is reduced below 10 ps, the BER curve tends to move away from the back-to-back. This can also be seen in Fig. 4(b), which shows the power penalty obtained at different differential delay. It can be seen that a delay of around 12 ps is optimal. As expected, the required differential delay correlates very well with our input pulsewidth of around 11 ps. A greater delay does

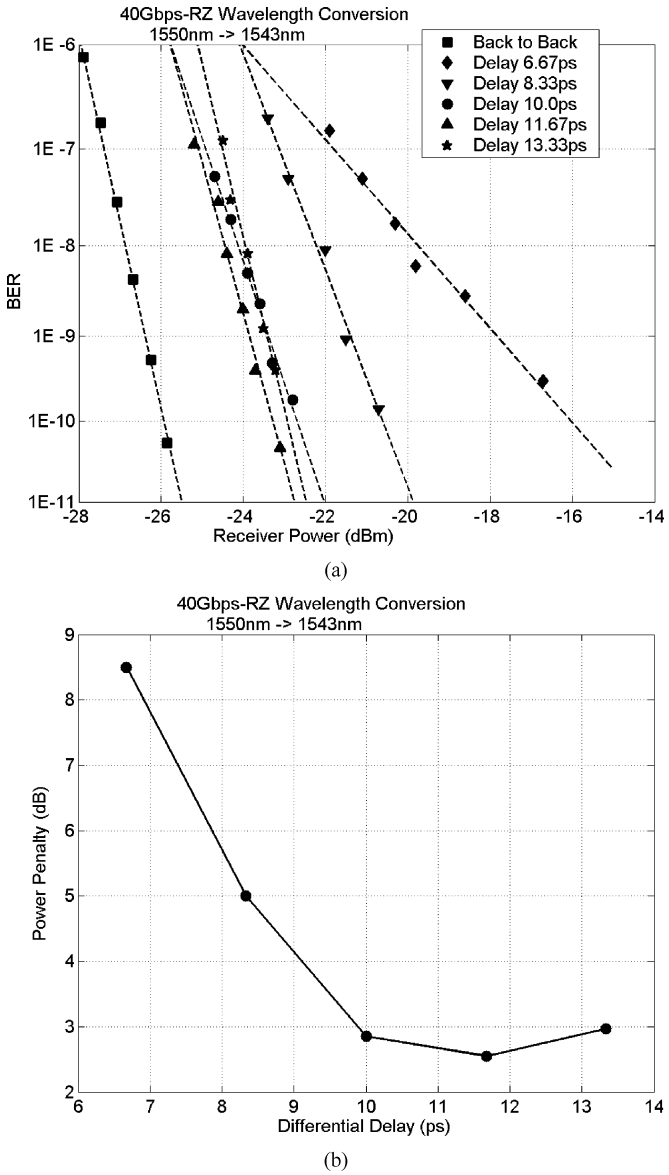

Fig. 4. (a) BER plots at 40-Gb/s operation for different differential delay. (b) Power penalty versus differential delay.

not cause any degradation, but as we move toward integrating the delay on-chip, we need to select the smallest possible delay to minimize the chip area and passive loss.

We also measured the performance of the device for different output wavelengths at 40-Gb/s data rates. The input power level required for our device was around 5 dBm in each input fiber and the output power was around -10 dBm in the output fiber. The OSNR of the output signal for a 1-nm optical bandwidth was 29 dB. The preamplifier SOAs were biased at around 80 mA to reduce the pattern effects and the MZI-SOAs were biased at 300 mA. We were able to operate the device from 1540 to 1565 nm, and obtain clear open eyes with an extinction ratio greater than 9 dB. Fig. 5 shows the output eye diagrams for a set of output wavelengths. The input wavelength was fixed at 1550 nm. The EDFAs and thin film filters in our device testing setup limited us to wavelengths below 1565 nm, even though the device itself can tune to wavelengths longer than 1565 nm.

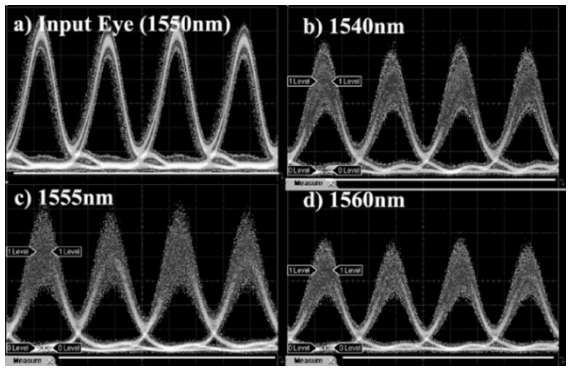

Fig. 5. A 40-Gb/s wavelength converter operation. (a) Input eye 1550 nm. (b)-(d) Converted eyes at different output wavelengths.

IV. Conclusion

In this letter, we demonstrated the 40-Gb/s operation of a monolithically integrated widely TAO-WC realized in an OQW platform. We characterized the effect of the differential delay and showed a power penalty, at $1E-9$ error rate, of less than 3 dB at the optimal delay. Error-free wavelength conversion was performed at 40-Gb/s RZ with an output extinction ratio $>$ 9 dB across a 25-nm output tuning.

The OQW platform allowed robust integration of active–passive components on-chip. This demonstration of high-speed wavelength conversion using OQW active-region-based devices and the characterization of the effect of the differential delay opens the way toward realizing more complex devices, both in terms of the integration process, and function. The next generation of these devices is currently being fabricated with the optimal delay integrated on-chip to realize a monolithic implementation.

References

[1] S. L. Danielsen, P. B. Hansen, and K. E. Stubkjaer, "Wavelength conversion in optical packet switching," *J. Lightw. Technol.*, vol. 16, no. 12, pp. 2095–2108, Dec. 1998.

[2] C. Joergensen, S. L. Danielsen, M. Vaa, B. Mikkelsen, K. E. Stubkjaer, P. Doussiere, F. Pommerau, L. Goldstein, and M. Goix, "40 Gbit/s alloptical wavelength conversion by semiconductor optical amplifiers," *Electron. Lett.*, vol. 32, pp. 367–368, 1996.

[3] B. Mikkelsen, K. S. Jepsen, M. Vaa, H. N. Poulsen, K. E. Stubkjaer, R. Hess, M. Duelk, W. Vogt, E. Gamper, E. Gini, P. A. Besse, H. Melchior, S. Bouchoule, and F. Devaux, "All-optical wavelength converter scheme for high speed RZ signal formats," *Electron. Lett.*, vol. 33, pp. 2137–2139, 1997.

[4] M. L. Nielsen, M. Nord, M. N. Petersen, B. Dagens, A. Labrousse, R. Brenot, B. Martin, S. Squedin, and M. Renaud, "40 Gbit/s standard mode wavelength conversion in all-active MZI with very fast response," *Electron. Lett.*, vol. 39, pp. 385–386, 2003.

[5] J. Leuthold, B. Mikkelsen, G. Raybon, C. H. Joyner, J. L. Pleumeekers, B. I. Miller, K. Dreyer, and C. A. Burrus, "All-optical wavelength conversion up to 100 Gbit/s with SOA delayed-interference configuration," in *26th Eur. Conf. Optical Communication*, vol. 3, 2000, pp. 119–20.

[6] M. L. Mašanović, V. Lal, J. A. Summers, J. S. Barton, E. J. Skogen, L. A. Coldren, and D. J. Blumenthal, "Design and performance of a monolithically-integrated widely-tunable all-optical wavelength converter with independent phase control," *IEEE Photon. Technol. Lett.*, vol. 16, no. 10, pp. 2299–2301, Oct. 2004.

[7] M. L. Mašanović, V. Lal, J. A. Summers, J. Barton, E. Skogen, L. Rau, L. Coldren, and D. Blumenthal, "Widely tunable monolithically integrated all-optical wavelength converters in InP," *J. Lightw. Technol.*, vol. 23, no. 3, pp. 1350–1362, Mar. 2005.